Accepted Manuscript

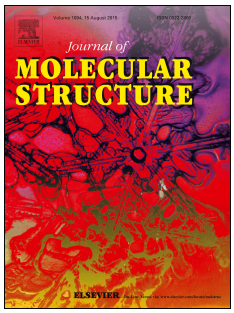

Synthesis, Molecular Structure and Spectroscopic Studies of Some New Quinazolin-4(3H)-one Derivatives; An Account on the N- versus S-Alkylation

Mohamed Hagar, Saied M. Soliman, Farahate Ibid, E.S.H. El Ashry

PII: S0022-2860(15)30496-8

DOI: 10.1016/j.molstruc.2015.12.007

Reference: MOLSTR 22040

To appear in: *Journal of Molecular Structure*

Received Date: 5 November 2015

Revised Date: 2 December 2015

Accepted Date: 2 December 2015

Please cite this article as: M. Hagar, S.M. Soliman, F. Ibid, E.S.H. El Ashry, Synthesis, Molecular Structure and Spectroscopic Studies of Some New Quinazolin-4(3H)-one Derivatives; An Account on the N- versus S-Alkylation, *Journal of Molecular Structure* (2016), doi: 10.1016/j.molstruc.2015.12.007.

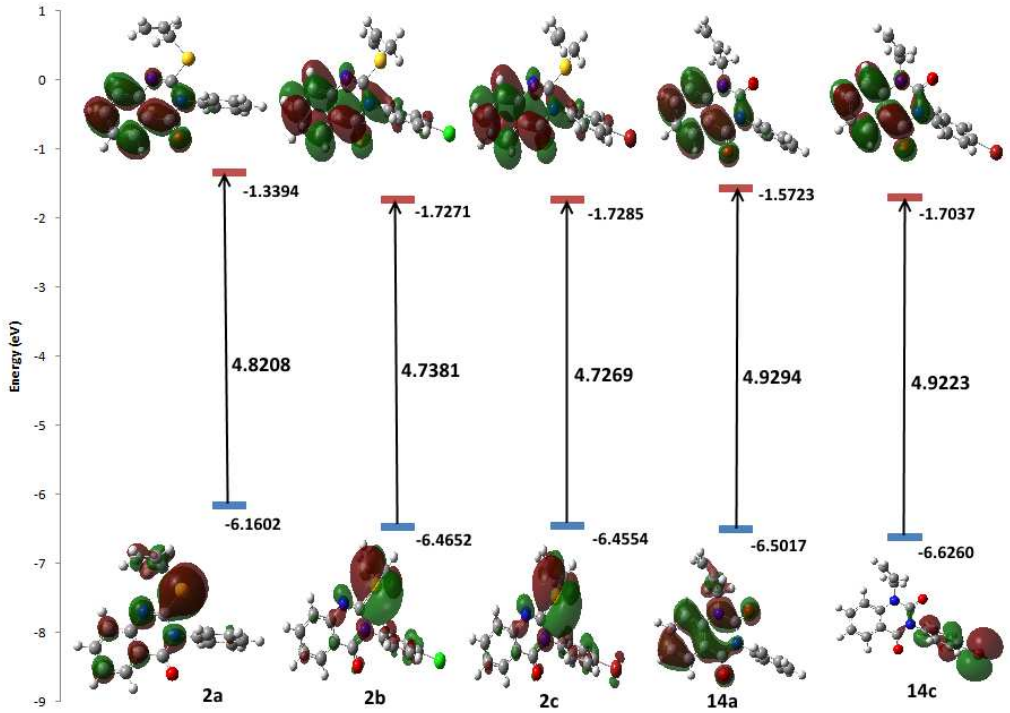

Synthesis, Molecular Structure and Spectroscopic Studies of Some New Quinazolin-4(3H)-one Derivatives; An Account on the N- versus S-Alkylation.

Mohamed Hagar[a,c], Saied M. Soliman [b,c], Farahate Ibid [c], E. S. H. El Ashry [c]*

a. *present address: Chemistry Department, Faculty of Science, Taibah University, Yanbu branch, Yanbu, KSA*

b. *present address: Chemistry Department, College of Science & Arts, King Abdulaziz University, P.O. Box 344 Rabigh 21911, Saudi Arabia*

c. *permanent address: Chemistry Department, Faculty of Science, Alexandria University, Alexandria, Ibrahimia, P.O. Box 426, Alexandria 21321. Egypt. E-mail*: eelashry60@hotmail.com

Abstract

A new series of N- and S-alkylated products of 3-aryl-1*H*,3*H*-quinazolin-2,4-dione and 3-aryl-2-mercapto-3H-quinazolin-4-one, respectively, were prepared in good yields via efficient nucleophilic substitution reaction of the SH and NH substrates with methyl iodide, ethyl bromoacetate, allyl bromide, propagyl bromide, 2-bromoethanol, 1,3-dibromopropane or phenacyl bromide in DMF as a solvent and anhydrous potassium carbonate. The quinazolin-2,4-dione favored the N-alkylation while the 2-mercapto-3H-quinazolin-4-one goes via the S-alkylation. DFT reactivity studies showed that the former have the N-site with higher nucleophilicity compared to the O-site. In contrast, the S-site is the more nucleophilic centre than the N-atom of the latter. The structures of the synthesized products have been established on the basis of their melting point (m.p), IR and ^{1}HNMR data. The molecular structures of the products were calculated using the DFT B3LYP/6-311G(d,p) method. The electronic and spectroscopic properties (Uv-Vis and NMR spectra) were calculated using the same level of theory. The chemical reactivity descriptors that could help to understand the biological activity of the products are also predicted.

Keywords: Quinazoline - DFT- S and N Alkylation- Reactivity

Introduction

4(3*H*)-Quinazolinones are a class of fused heterocycles that of considerable interest because of the diverse range biological properties, such as anticancer, diuretic, anti-inflammatory, anticonvulsant and antihypertensive activities [1-5]. Some of aminoquinazoline derivatives were found to be inhibitors of the tyrosine kinase [6, 7] or dihydrofolate reductase enzymes [8]. The chemistry of the quinazolinone alkaloids is well documented [9, 10] in a number of comprehensive reviews and monographs which is continuously updated in Natural Product Reports [11, 12]. Recently, it was reported that substituted quinazolines exhibited a good antibacterial activity [13]. Prompted by these findings and continuing our interests devising approaches for the preparations of heterocycles of potential biological activities, the aim of this work is mainly concerned with studying the activity of N and S of quinazolin-4(3H)-one derivatives towards alkylation reactions as well as the design and synthesis of an extension series of quinazolin-4(3H)-one derivatives. Also, the molecular structures, electronic and spectroscopic properties of the products were calculated using the DFT method.

Experimental

General Methods

IR spectral data were recorded with a Tensor 37 Bruker infrared spectrophotometer (KBr, ν max: cm^{-1}). Mass spectra were recorded at 70 ev by 5980 series II GC coupled with 5989 B mass spectrometer. ^{1}H NMR spectra were determined with a JEOL spectrometer at 500 MHz. The ^{13}C NMR spectra were recorded with JEOL spectrometer at 125.7 MHz. The chemical shifts are expressed in the δ scale using tetramethylsilane as a reference. Melting points were determined on a meltemp apparatus and are uncorrected. TLC was performed on Merck Kiesel gel; 60-F254 plates, and the spots were detected by UV light absorption.

General method for synthesis of 2-(alkylthio)-3-(aryl)quinazolin-4(3H)-one (2-5)

A mixture of 3-aryl-2-mercaptoquinazolin-4(1*H*, 3*H*)-one **1a-c** (0.78 mmol) and anhydrous potassium carbonate (0.8 mmol) in dry DMF (3 mL) was stirred for 1hr, alkyl halide (0.78 mmol) was added. The reaction mixture was stirred for further time 10:120 min and then diluted with cold water. The formed precipitate was filtered, washed with water and recrystallized from ethanol.

2-(Allylthio)-3-phenylquinazolin-4(3H)-one (2a)

Stirring time 5 min, colorless crystals; yield: 67 %; mp 147-148 °C [14].

2-(Allylthio)-3-(4-chlorophenyl)quinazolin-4(3H)-one (2b)

Stirring time 30 min, colorless needles; yield: 78 %; mp 138-140 °C, R_f 0.54 (1:6 EtOAc-hexane). ^{1}H NMR (500 MHz, $CDCl_3$): δ = 3.84 (d, 2H, J = 6.7 Hz, CH_2S), 5.14 (d, 1H, J = 9.5 Hz, CH-All), 5.30 (d, 1H, J = 1.9 Hz, CH-All), 5.91 (m, 1H, CH-All), 7.25 (d, 2H, J = 8.6 Hz, Ar-H), 7.40 (t, 1H, J = 7.6 Hz, Quin-H), 7.50 (d, 2H, J = 8.6 Hz, Ar-H), 7.61 (d, 1H, J = 7.6 Hz, Quin-H), 7.73 (t, 1H, J = 6.7 Hz, Quin-H), 8.22 (d, 1H, J = 6.7 Hz, Quin-H). ^{13}C NMR (125.7 MHz, $CDCl_3$): δ = 35.5 (SCH_2), 119.8 (CH_2═), 126.0 (C-4a), 127.2 (C-5), 127.4 (C-8), 130.0 (C-6), 132.6 (CH═), 136.2 (C-7), 147.7 (C-8a), 156.4 (C-2), 161.8 (C-4). Anal. Calcd for $C_{17}H_{13}ClN_2OS$: C, 62.10; H, 3.98; N, 8.52; S, 9.75. Found C, 61.98; H, 3.61; N, 8.23; S, 9.40.

2-(Allylthio)-3-(4-bromophenyl)quinazolin-4(3H)-one (2c)

Stirring time 60 min, colorless crystals; yield: 92%; mp 202-204 °C [15].

2-(1-Oxo-1-phenylethylthio)-3-phenylquinazolin-4(3H)-one (3a)

Stirring time 120 min, yellow needles; yield: 55%; mp 201-203°C, R_f 0.38 (1:2 EtOAc- petrolum ether). IR (KBr, in cm^{-1}): 3060 (CH-Ar), 2910 (CH alkane), 1689 (CO), 1608 (CON), 1574 (C=N), 1547 (C=C). ^{1}H NMR (500 MHz, $CDCl_3$): δ = 4.64 (s, 2H, SCH_2), 7.28 (d, 1H, J = 8.4 Hz, Ar-H), 7.37 (m, 3H, Ar-H), 7.55 (m, 5H, Ar-H), 7.63 (dd, 2H, J_1 = J_2 = 8.4 Hz, Ar-H), 8.09 (d, 2H, J = 6.9 Hz, Ar-H), 8.20 (d, 1H, J = 7.6 Hz, Ar-H). ^{13}C NMR (125.7 MHz, $CDCl_3$): δ = 39.9 (SCH_2), 119.8 (C-4a), 126.2 (C-5), 127.4 (C-6), 147.2 (C-8a), 156.7 (C-2), 161.6 (C-4), 193.5 (CO). Anal. Calcd for $C_{22}H_{16}N_2O_2S$: C, 70.95; H, 4.33; N, 7.52; S, 8.61. Found C, 71.14; H, 4.52; N, 7.45; S, 8.32.

2-(1-Oxo-1-phenylethylthio)-3-(4-chlorophenyl)quinazolin-4(3H)-one (3b)

Stirring time 30 min, colorless needles; yield: 82.1%; mp 213-215 °C, R_f 0.46 (1:2 EtOAc-petrolum ether). IR (KBr, in cm^{-1}): 3064 (CH-Ar), 2912 (CH alkane), 1774 (CO), 1606 (CON), 1596 (C=N), 1490 (C=C). ^{1}H NMR (500 MHz, $CDCl_3$): δ = 4.64 (s, 2H, SCH_2), 7.28 (d, 1H, J = 7.6 Hz, Ar-H), 7.33 (d, 2H, J = 8.4, Ar-H), 7.37 (t, 1H, J = 7.6, Ar-H), 7.53 (dd, 4H, J = 6.9 Hz, Ar-H), 7.64 (dd, 2H, J_1 = J_2 = 7.6 Hz, Ar-H), 8.08 (d, 2H, J = 7.6 Hz, Ar-H), 8.18 (d, 1H, J = 7.6 Hz, Ar-H). ^{13}C NMR (125.7 MHz, $CDCl_3$): δ = 40.1 (SCH_2), 119.6 (C-4a), 126.2 (C-6), 127.3 (C-5), 147.1 (C-8a), 156.3 (C-2), 161.5 (C-4). Anal. Calcd for $C_{22}H_{15}ClN_2O_2S$: C, 64.94; H, 3.72; N, 6.88; S, 7.88. Found C, 65.17; H, 3.58; N, 6.61; S, 7.54.

2-(1-Oxo-1-phenylethylthio)-3-(4-bromophenyl)quinazolin-4(3H)-one (3c)

Stirring time 60 min, colorless needles; yield: 74 %; mp 222-224 °C, R_f 0.42 (1:2.5 EtOAc-hexane). IR (KBr, in cm^{-1}): 3064 (CH-Ar), 2914 (CH alkane), 1772 (CO), 1606 (CON), 1596 (C=N), 1488 (C=C). ^{1}H NMR (500 MHz, $CDCl_3$): δ = 4.66 (s, 2H, SCH_2), 7.26 (d, 1H, J = 8.4 Hz, Ar-H), 7.29 (d, 2H, J = 8.4, Ar-H), 7.37 (t, 1H, J = 7.6, Ar-H), 7.53 (t, 2H, J = 7.6 Hz, Ar-H), 7.64 (dd, 2H, J_1 = J_2 = 7.6 Hz, Ar-H), 7.70 (d, 2H, J = 8.4 Hz, Ar-H), 8.08 (d, 2H, J = 7.6 Hz, Ar-H), 8.18 (d, 1H, J = 7.6 Hz, Ar-H). ^{13}C NMR (125.7 MHz, $CDCl_3$): δ = 40.2 (SCH_2), 119.7 (C-4a), 126.7 (C-5), 127.3 (C-5), 146.9 (C-8a), 156.3 (C-2), 161.4 (C-4), 193.4 (CO).

2-(2-Hydroxyethylthio)-3-phenylquinazolin-4(3H)-one (4a)

Stirring time 20 min, colorless needles; yield: 68 %; mp 129-131 °C, R_f 0.37 (1:1.5 EtOAc- petrolum ether). IR (KBr, in cm^{-1}): 3270 (OH), 3058 (CH-Ar), 2936 (CH alkane), 1608 (CON), 1573 (C=N), 1479 (C=C). ^{1}H NMR (500 MHz, DMSO-d_6): δ = 3.22 (t, 2H, J = 6.1 Hz, SCH_2), 3.60 (q, 2H, J = 6.1 Hz, CH_2OH), 4.94 (t, 1H, J = 5.3 Hz, OH), 7.41 (m, 2H, Ar-H), 7.44 (d, 1H, J = 6.9 Hz, Ar-H), 7.54 (m, 3H, Ar-H), 7.57 (d, 1H, J = 8.4 Hz, Ar-H), 7.80 (m, 1H, Ar-H), 8.04 (dd, 1H, J_1 = 8.4 Hz, J_2 = 1.5 Hz, Ar-H). Anal. Calcd for $C_{16}H_{14}N_2O_2S$: C, 64.41; H, 4.73; N, 9.39; S, 10.75. Found C, 64.86; H, 4.51; N, 9.04; S, 10.52.

2-(2-Hydroxyethylthio)-3-(4-chlorophenyl)quinazolin-4(3H)-one (4b)

Stirring time 120 min, colorless needles; yield: 86.3%; mp 165-167 °C [15].

2-(2-Hydroxyethylthio)-3-(4-bromophenyl)quinazolin-4(3H)-one (4c)

Stirring time 60 min, colorless needles; yield: 87%; mp 184-185 °C, R_f 0.63 (1:2 EtOAc- petrolum ether). IR (KBr, in cm^{-1}): 3566 (OH), 3062 (CH-Ar), 2938(CH alkane), 1606 (CON), 1574 (C=N), 1486 (C=C), 530 (C-Br). ^{1}H NMR (500 MHz, DMSO-d_6): δ = 3.23 (t, 2H, J = 6.1 Hz, SCH_2), 3.60 (q, 2H, J = 6.1 Hz, CH_2OH), 4.94 (t, 1H, J = 5.3 Hz, OH), 7.42 (d, 2H, J = 8.4 Hz, Ar-H), 7.44 (d, 1H, J = 7.6 Hz, Ar-H), 7.57 (d, 1H, J = 8.4 Hz, Ar-H), 7.74 (d, 2H, J = 8.4 Hz, Ar-H), 7.80 (m, 1H, Ar-H), 8.03 (d, 1H, J = 6.9 Hz, Ar-H). Anal. Calcd for $C_{16}H_{13}BrN_2O_2S$: C, 50.94; H, 3.47; N, 7.43; S, 8.50. Found C, 51.09; H, 3.66; N, 7.72; S, 8.61.

General method for acid hydrolysis of (12a-c)

A solution of (0.91 mmol) of **9a-c** and conc HCl (6mL) was warmed in water path for 1hr, then the reaction mixture was poured into water. The formed precipitate was filtered, washed with water and recrystalized from ethanol.

3-Phenylquinazoline-2,4(1H,3H)-dione (12a)

colorless crystals; yield: 82 %; mp 281-283 °C, R_f 0.43 (1.5:1 EtOAc- petrolum ether). ^{1}H NMR (500 MHz, DMSO-d_6): 7.19 (dd, 2H, J_1 = 7.6, J_2 = 6.9, Ar-H), 7.29 (d, 2H, J = 8.4 Hz, Ar--H), 7.39 (dd, 2H, J_1 = 7.6, J_2 = 6.9, Ar-H), 7.45 (dd, 2H, J_1 = 8.4, J_2 = 6.9, Ar-H), 7.67 (dd, 2H, J_1 = 8.4, J_2 = 6.9, Ar-H), 7.90 (d, 1H, J = 8.4 Hz, Ar-H), 11.53 (s, 1H, NH).

3-(4-Phlorophenyl)quinazoline-2,4(1H,3H)-dione (12b)

Colorless crystals; yield: 88 %; mp 299-300 °C, R_f 0.63 (1:2.5 EtOAc- petrolum ether). ^{1}H NMR (500 MHz, DMSO-d_6): 7.22 (m, 2H, Ar-H), 7.37 (d, 2H, J = 15 Hz, Ar-H), 7.54 (d, 2H, J = 15 Hz, Ar-H), 7.70 (m, 1H, Ar-H), 7.93 (d, 1H, J = 11.5 Hz, Ar-H), 11.55 (s, 1H, NH), m/z: 272.

3-(4-Bromophenyl)quinazoline-2,4(1H,3H)-dione (12c)

Colorless crystals; yield: 91 %; mp 326-328 °C, R_f 0.38 (1:1 EtOAc- petrolum ether). IR (KBr, in cm^{-1}): 3455 (NH), 1669 (CON), 1581 (C=N), 1515 (C=C). ^{1}H NMR (500 MHz, DMSO-d_6): 7.18 (m, 2H, Ar-H), 7.28 (d, 2H, J = 8.4 Hz, Ar-H), 7.66 (m, 3H, Ar-H), 7.90 (d, 1H, J = 8.4, Ar-H), 11.56 (s, 1H, NH).

General procedure for alkylation reaction of 3-arylquinazolin-2,4(1*H*,3*H*)-dione

A mixture of **12a-c** (0.6 mmol) and anhydrous potassium carbonate (0.9 mmol) in dry DMF (3 mL) was stirred for 1hr, appropriate alkyl halide (0.6 mmol) was added. The reaction mixture was stirred for further time 10:60 min, then diluted with cold water. The formed precipitate was filtered, washed with water and recrystallized from ethanol

1-Methyl-3-phenylquinazoline-2,4(1H,3H)-dione (13a)

Stirring time 30 min, colorless needles; yield: 91 %; mp 220-221°C. ^{1}H NMR (500 MHz, $CDCl_3$): δ = 3.64 (s, 3H, CH_3), 7.28 (m, 4H, Ar-H), 7.44 (dd, 1H, J_1 = 7.6 Hz, J_2 = 6.9 Hz, Ar-H), 7.51 (dd, 2H, J_1 = 8.4 Hz, J_2 = 6.9 Hz, Ar-H), 7.73 (m, 1H, Ar-H), 8.62 (dd, 1H, J_1 = 7.6 Hz, J_2 = 1.5 Hz, Ar-H).

1-Methyl-3-(4-Chlorophenyl)quinazolin-2,4(1*H*,3*H*)-dione (13b)

Stirring time 20 min, colorless crystals; yield: 99 %; mp 223-225°C. IR (KBr, in cm^{-1}): 2982 (CH alkane), 1707 (NCON), 1661 (CON), 1482 (C=C), 761 (C-Cl). ^{1}H NMR (500 MHz, $CDCl_3$): δ = 3.63 (s, 3H, CH_3), 7.21 (d, 2H, J = 8.4 Hz, Ar-H), 7.28 (m, 2H, Ar-H), 7.47 (d, 2H, J = 8.4, Ar-H), 7.74 (m, 1H, Ar-H), 8.25 (m, 1H, Ar-H). m/z 286.

1-Methyl-3-(4-bromophenyl)quinazolin-2,4(1*H*,3*H*)-dione (13c)

Stirring time 15 min, colorless crystals; yield: 90 %; mp 214-216 °C. IR (KBr, in cm^{-1}): 3062 (CH alkane), 1657 (CON), 1715 (NCON), 1481 (C=C), 515 (C-Br). ^{1}H NMR (500 MHz, $CDCl_3$): δ = 3.63 (s, 3H, CH_3), 7.15 (d, 2H, J = 8.4 Hz, Ar-H), 7.28 (m, 2H, Ar-H), 7.63 (d, 2H, J = 8.4, Ar-H), 7.74 (m, 1H, Ar-H), 8.25 (dd, 1H, J_1 = 7.6 Hz, J_2 = 1.5 Hz, Ar-H).

1-Allyl-3-phenylquinazolin-2,4(1*H*,3*H*)-dione (14a)

Stirring time 30 min, colorless needles; yield: 91 %; mp 160-161 °C, R_f 0.59 (1:1 EtOAc-hexane). IR (KBr, in cm^{-1}): 2901 (CH-Ar), 2987 (CH alkene), 1706 (NCON), 1655 (CON), 1478 (C=C). ^{1}H NMR (500 MHz, $CDCl_3$): δ = 4.80 (d, 2H, J = 4.6 Hz, NCH_2), 5.29 (m, 2H, CH_2═), 5.96 (m, 1H, CH═), 7.26 (m, 4H, Ar-H), 7.44 (dd, 1H, J_1 = 7.6 Hz, J_2 = 6.8 Hz, Ar--H), 7.51 (dd, 2H, J_1 = 8.4 Hz, J_2 = 6.8 Hz, Ar-H), 7.69 (m, 1H, Ar-H), 8.26 (m, 1H, Ar-H). ^{13}C NMR (125.7 MHz, $CDCl_3$): δ = 46.2 (NCH_2), 114.0 (C-8), 118.1 (CH_2═), 122.8 (C-4a), 128.0 (C-6), 128.8 (C-5), 129.5 (CH═), 131.2 (C-7), 140.2 (C-8a), 150.9 (C-2), 161.9 (C-4). Anal. Calcd for $C_{17}H_{14}N_2O_2$: C, 73.37; H, 5.07; N, 10.07. Found C, 73.18; H, 5.28; N, 10.27.

1-Allyl-3-(4-chlorophenyl)quinazolin-2,4(1*H*,3*H*)-dione (14b)

Stirring time 20 min, colorless needles; yield: 96 %; mp 156-157 °C, R_f 0.62 (1:1 EtOAc-hexane). IR (KBr, in cm^{-1}): 3089 (CH-Ar), 3064 (CH alkene), 2988 (CH alkane), 1722 (NCON), 1666 (CON), 1479 (C=C), 759 (C-Cl). ^{1}H NMR (500 MHz, DMSO-d_6): δ = 4.72 (d, 2H, J = 3.4 Hz, NCH_2), 5.29 (2d, J_1 = 17.2 Hz, J_2 = 10.3 Hz, 2H, CH_2═), 5.90 (m, 1H, CH═), 7.28 (dd, 1H, J_1 = 8.0 Hz, J_2 = 6.9 Hz, Ar-H), 7.37 (dd, 3H, , J_1 = 8.5 Hz, J_2 = 8.0 Hz, Ar--H), 7.52 (d, 2H, J = 8.5 Hz, Ar-H), 7.75 (m, 1H, Ar-H), 8.03 (m, 1H, Ar-H). ^{13}C NMR (125.7 MHz, DMSO-d_6): δ = 45.8 (NCH_2), 115.8 (C-8), 116.1 (CH_2═), 122.9 (C-4a), 123.7 (C-6), 128.7 (C-5), 129.2 (CH═), 131.6 (C-7), 140.5 (C-8a), 150.6 (C-2), 161.8 (C-4), m/z: 312.1. Anal. Calcd for $C_{17}H_{13}ClN_2O_2$: C, 65.29; H, 4.19; N, 8.96.. Found C, 65.58; H, 4.01; N, 8.72.

1-Allyl-3-(4-bromophenyl)quinazolin-2,4(1*H*,3*H*)-dione (14c)

Stirring time 15 min, colorless needles; yield: 92 %; mp 177-179 °C, R_f 0.14 (1:1.5 EtOAc-hexane). IR (KBr, in cm^{-1}): 3087 (CH-Ar), 3058 (CH-Ar), 3063 (CH alkene), 2936 (CH alkane), 1722 (NCON), 1662 (CON), 1479 (C=C), 514 (C-Br). ^{1}H NMR (500 MHz, $CDCl_3$): δ = 4.79 (d, 2H, J = 5.2 Hz, NCH_2), 5.29 (m, 2H, CH_2-All), 5.95 (m, 1H, CH-All), 7.16 (d, 2H, J = 8.4 Hz, Ar-H), 7.26 (m, 2H, Ar--H), 7.62 (d, 2H, J = 8.4 Hz, Ar-H), 7.69 (m, 1H, Ar-H), 8.25 (m, 1H, Ar-H). ^{13}C NMR (125.7 MHz,

$CDCl_3$): δ = 46.3 (NCH_2), 114.1 (C-8), 118.2 (CH_2═), 123.7 (C-4a), 129.4 (C-6), 129.8 (C-5), 130.7 (CH═), 131.5 (C-7), 140.1 (C-8a), 150.6 (C-2), 161.7 (C-4).

Computational details

All the quantum chemical calculations of the studied compounds were performed by applying DFT method with the B3LYP functional and 6–311G(d,p) basis set using Gaussian 03 software [16]. The geometries were optimized by minimizing the energies with respect to all the geometrical parameters without imposing any molecular symmetry constraints. GaussView 4.1 [17] and Chemcraft [18] programs have been used to draw the structure of the optimized geometry. The computational study of the reactant species was first carried out in gas phase, then, the Self-Consistent Reaction Field (SCRF) theory [19], with Polarized Continuum Model (PCM) was used to predict the effect of solvent (DMSO) on the stability of the tautomers studied [20]. The natural atomic charges are calculated using NBO calculations as implemented in the Gaussian 03 package [21] at the DFT/B3LYP level. The nucleophilicity index [21] is calculated referred to tetracyanoethylene (TCE) is given by

$$N = E_{HOMO(Nu)} - E_{HOMO(TCE)} \qquad (5)$$

Fukui functions for electrophilic attack on an atom, k, in an N-electron system was introduced by Yang and Mortier [8] as

$$f_k^- = q_k(N) - q_k(N-1) \qquad (7)$$

where $q_k(N)$ and $q_k(N-1)$ are the atomic charges of the system with N and N-1 electrons, respectively. The condensed Fukui functions f_k^- are calculated using Natural population analysis (NPA) [23].

Condensed local nucleophilicity index (N_k) [24] is defined

$$N_k = f_k^- N \qquad (9)$$

Also the molecular structures of the products **2a-c**, **14a** and **14c** were calculated using the same level of theory. The electronic and spectroscopic properties of the selected products were also predicted.

Results and discussion

The starting materials 3-aryl-2-mercapto-3H-quinazolin-4-one **1a-c** were prepared adopting the reported procedure [25]. The 2-mercapto group of **1a-c** was alkylated with a variety of alkyl halides, methyl iodide, allyl bromide, phenacyl bromide and 2-bromoethanol in DMF as a solvent and anhydrous potassium carbonate to give the

thio-ether derivatives, (scheme 1). The structures of the products were confirmed by their spectral data.

The treatment of the ester **5a-c** with hydrazine hydrate afforded the corresponding hydrazide **9a-c** [26, 27]. The reaction of **9a-c** with ammonium mercaptocyanate failed to give **10** neither in aqueous HCl nor in benzene as a solvent [28] while the reaction in aqueous HCl proceeds to give 3-aryl-1*H*,3*H*-quinazolin-2,4-dione **12a-c** instead. The yield of **12a-c** is improved from 42 % in dilute HCl to 91% in concentrated HCl. The structure was confirmed by IR spectroscopy which showed absence of peaks at 3303 cm^{-1} corresponding to NH_2 group of **9**. The mass spectrum of **12b** showed the molecular ion peak at m/z 272.

The NH-group of **12a-c** was alkylated with a series of alkyl halides, methyl iodide and allyl bromide using potassium carbonate in DMF to give **13a-c** and **14a-c**, respectively. The structures of these compounds were confirmed by their spectral data.

It is clear that the reactants **1a-c** and **12a-c** could undergo the tautomeric equilibrium reactions shown in scheme 3. The relative stability as well as chemical reactivity of these tautomers in gas phase and in solution have been predicted using DFT/B3LYP method. The alkylation reaction of the thiones (**1a-c**) proceeds to the formation of the S-alkylated products whatever the alkyl halide used. In these cases, the attack occurs on the S-atom rather than the ring N-atom of the heterocycle. In contrast, the diones **12a-c** yielded the N-alkylated products via the attack of the alkyl halide on quinazoline ring nitrogen instead of the carbonyl O-atom, hence N-alkylated products were obtained. In this section the stability of the possible tautomers will be investigated in the framework of the DFT method followed by studying the chemical reactivity, site reactivity and selectivity towards these alkylation reactions using the well known quantum chemical descriptors described above.

Stability of the studied tautomers

The relative stabilities and the population of these isomers are predicted using B3LYP/6-311G(d,p) calculations. The B3LYP/6-311G(d,p) calculated energy predictions of the studied tautomers are compared in Table S1 (Supplementary Materials) which shows that T1 tautomers have lower energy values than T2 in all cases. The relative abundance of the studied tautomers was calculated from: $\Delta G = -RT\ln K$, where ΔG denotes the difference between the Gibbs free energies of a given isomer relative to the most stable one and K is the corresponding equilibrium

constant. The abundance of the most stable species, T1 tautomer equal ~100.00% at 298 K in the gas phase. The T2 forms have zero total populations and are expected to be of no importance. Because the solvent effects are important in tautomer stability phenomena as the polarity differences among isomers can make significant changes in their relative energies in solution so we used PCM to model the effect of solvent on these tautomeric equilibrium reactions. Table S2 (Supplementary Information) showed the total energies and thermodynamic parameters of the studied isomers in presence of DMSO as solvent. The effect of solvent on the calculated energies and thermodynamic parameters is shown in Table S2 (Supplementary Information). In solution, the energy barrier (ΔE) between the two tautomers increased compared to the gas phase. It is revealed that the stability of T1 increases in presence of solvent. Anyway the most stable isomer T1 is almost the only species that could exist in solution where the T2 has almost null population.

Reactivity and site selectivity of the reactants

For the studied substrates, the calculated quantum chemical descriptors such as E_{HOMO}, E_{LUMO} and nucleophilicity index (N) obtained at the DFT/B3LYP/6-311G(d,p) level of theory are collected in Table 1. The atomic charge densities at the N- and S-sites of the N (Q_N) and N-1 (Q_{N-1}) systems were calculated and presented in Table 2. The calculated local nucleophilicity trend of the studied substrates is analyzed using local nucleophilicity index N_k and Fukui function f_k^-. The values of these local reactivity descriptors on the N- and S-atoms of compounds **1a-c** and **12a-c** are given in Table 2. The most significant results that can be easily concluded from Table 1 is the lower nucleophilicity index values for compounds **b** and **c** due to the presence of the halogen substitution at the phenyl ring. The nucleophilicity index has maximum values for compounds **a**. In a number of studies, NPA charges are usually used for f_k^- calculations where the atomic centers with maximal f_k^- are interpreted as the most reactive nucleophilic reaction sites [29-32]. For compounds **1a-c**, the N_k and f_k^- values are higher for the S-sites compared to the N-one. These results indicated the higher reactivity of the S-site towards nucleophilic attack compared to the N-site, hence S-alkylated products were obtained. In contrast, the compounds **12a-c** have N-atom with higher nucleophilicity index N_k and Fukui function f_k^- values than the O-atom. The N-alkylation is the best option for **12**. From this point of view we could conclude that, the compounds **1a-c** favor the S-alkylation while the **12a-c** favor the N-alkylation reaction.

Modeling the structure of the products:

The optimized structures of the products **2a-c**, **14a** and **14c** were calculated using 6-311G(d,p) level of theory which used as models to describe the geometric structure of the obtained products. The optimized geometry of these compounds are shown in Fig.1. The optimized geometric parameters (bond distances and bond angles) were compared with the X-ray structure of the structurally related compounds [33,34] and the results were collected in Table 3. The results showed a good agreement between the calculated geometric parameters and the experimental data. It is worthnoting that, the quinazoline and phenyl rings are planar. The angle between the plane passing through the quinazoline ring and the plane passing through the phenyl ring is 88.3º, 69.4º and 68.88º for compounds **2a-c**, respectively. Moreover, the angle between the two ring planes in case of **14a** and **14c** is 85.5 and 80.1, respectively. The two rings are perpendicular to one another in compounds **a** where there is no substituent at the phenyl ring. The presence of large size halogen (Br) at the phenyl ring make the angle between the two ring planes becomes less compared to the unsubstituted derivatives, **a** i.e, more deviation from the perpendicularity of the two rings takes place. On other hand the R-groups are not coplanar with the quinazoline ring plane for all the studied compounds.

The charge calculations at different atomic sites play a crucial role in different properties such as dipole moment, molecular polarizability as well as electronic structure of a compound [35]. In this regard, the natural atomic charges (NAC) were calculated using NBO method at the DFT B3LYP/6-311G(d,p) level of theory and the results are given in Table 4. The natural charge calculations indicate the electronegative nature of the O and N-atoms. The maximum natural charges occur at the O-atoms for all the studied compounds (-0.5864 to -0.6247). All the carbon atoms are negative except those attached to strong electronegative atoms (O or N atoms). The most positively charged carbon atoms are C4, C8, C10 and C13 for compounds **2** and C4, C8, C10 and C12 for **14**. The maximum positive charge occurs at C10 for the former and C8 for the latter. The reason is that these C-atoms bonded to larger number of strong electronegative atoms. All H-atoms have positive charge densities. The halogen substiuent showed very little effect on the natural charge of the different atomic sites. Only we noted significant increase in the natural charge values at C16 and C15 of compounds **2b-c** and **14c** compared to **2a** and **14a**, respectively. The

electron withdrawing character of the halogen (Cl or Br) increase the natural charge value at the C-atom bonded to it compared to compounds **a**.

The dipole moments and polarizability of the studied systems are given in Table 5. It could be seen that the dipole moment is in the order **14c**>**14a**>**2a**>**2b**>**2c**. The polarity of the compounds **14** is higher due to the presence of one more O-atom while those having S-atom are less polar compounds. Significantly, the presence of the thione O-atom and the Br-atom in the same direction is a reasonable factor for the highest polarity predicted for **14c**. It seems that, the presence the hydrophobic moiety bonded to the S-atom in case of compounds **2** in the same direction with the halogen tends to decrease the polarity of the mercapto products. Polarizability depends on how the tendency of electron cloud of molecular system to distort under the effect of approaching charge. In fact, this depends on the structure complexity as well as the size of the molecular system. Molecules having large size are more polarizable. We noted that combination of S- and Br-atom in the same molecule leads to show the highest polarizability (**2c**).

Frontier molecular orbitals

For chemists and physicist, the properties of the frontier molecular orbitals (FMOs) like energy and electron densities are very important quantum chemical parameters. The electron densities of these FMOs were used for predicting the most reactive position in π–electron systems and also explained several types of reactions in conjugated system [36]. Moreover, the energies of the lowest unoccupied molecular orbital (E_{LUMO}) and the highest occupied molecular orbital (E_{HOMO}) and their energy gap (ΔE) reflect the chemical reactivity of the molecule. A molecule having high frontier orbital gap (ΔE) is less polarizable and is generally associated with a low chemical reactivity and high kinetic stability [37]. Recently, the energy gap between HOMO and LUMO has been used to prove the bioactivity from intramolecular charge transfer (ICT) [38, 39]. The E_{HOMO}, E_{LUMO} and ΔE values of the studied compound were calculated by B3LYP/6–311G(d,p) method. The HOMO and LUMO pictures are shown in Fig. 2. For compounds **2**, the electron densities of the HOMO and LUMO are mainly localized on the S-atom. The electron density of the HOMO level on the quinazoline ring is less significant in case of **2b** and **2c**. For compounds **14**, the HOMO is located on the quinazoline and phenyl rings for **a** and **c**, respectively. The LUMO of all the studied systems is mainly localized on the π-system of the quinazoline ring.

In general, the presence of halogen substituent on the phenyl ring stabilizes both HOMO and LUMO levels. The LUMO is stabilized further in comparison with HOMO, hence the energy gap decreased. For compounds **2**, the energy gap is in the order **a**>**b**>**c**. The molecule (**2a**) has highest energy gap (4.8208 eV). The presence of Br-atom attached to the phenyl ring enhances the ability of the system towards electron transfer process hence **2c** is the most polarizable due to the presence of combination of S and Br-atoms. In comparison, the oxo compounds **14a** and **14c** has higher energy gap compared to **2a** and **2c**, respectively. It is the maximum for **14a** which showed the maximum kinetic stability.

Based on the energies of the frontier molecular orbitals, various chemical reactivity descriptors such as electronegativity (χ), chemical potential (μ), chemical hardness (η), global softness (S) and global electrophilicity index (ω) [40-44] were proposed for understanding the different pharmacological aspects of drug molecules. These descriptors are calculated using Eqs (1)-(5) given below:

$$\chi = \frac{(I+A)}{2} \qquad 1$$

$$\mu = -\chi = -\frac{(I+A)}{2} \qquad 2$$

$$\eta = \frac{(I-A)}{2} \qquad 3$$

$$S = \frac{1}{2\eta} \qquad 4$$

$$\omega = \frac{\mu^2}{2\eta} \qquad 5$$

The chemical hardness is a measure of the resistance to charge transference [45], while the electronegativity is a measure of the tendency to attract electrons in a chemical bond, as is defined as the negative of the chemical potential in DFT [45]. Moreover, the electrophilicity index (ω) measures the stabilization in energy when the system acquires an additional electronic charge from the environment. It contains information about both electron transfer (chemical potential) and stability (hardness) and is a better descriptor of global chemical reactivity (Eq. 5). For the studied compounds, these chemical reactivity descriptors are given in Table 6. It is seen that all the studied systems have negative chemical potential and it means that the compounds are stable. The hardness signifies the resistance towards the deformation of electron cloud of chemical systems under small perturbation encountered during chemical process. Soft systems are large and highly polarizable, while hard systems are relatively small and much less polarizable. It is found that the compound (14**a**) is

the hardest while 2c is the softest. Moreover, the high value of electrophilicity index (ω) of **2**c favors its electrophilic behavior to be the highest [46].

Electronic spectra and TD-DFT calculations

The lowest energy electronic transition implies the electron transfer from the highest occupied molecular orbital (HOMO) to the lowest unoccupied molecular orbital (LUMO). The easiest way, but the less accurate, to calculate the energy of this transition is to calculate the energy gap between HOMO and LUMO levels. The calculated transition energy of the studied molecules are shown in Fig. 2. To get the accurate electronic transitions, we performed the time–dependant density functional theory (TD–DFT) calculations. The TD-DFT results of the spin allowed singlet-singlet electronic transitions collected in Table S3 (Supplementary Information). The most important electronic transition bands are shown in Table 7 while the theoretical spectra are shown in Fig. 3. Compound **2a** showed two electronic transition bands at 295.4 nm (f=0.0559) and 273.0 (f=0.1968) due to the H→L (87%) and H→L+1 (75%) transitions, respectively. These bands showed significant bathochromic shift in case of **2b** and **2c**. On other hand the longest wavelength band for **14c** at 289.1nm (f=0.0701) which is mainly due to H→L (85%) excitation showed slight bathochromic shift in presence of halogen substitution at the ring.

Molecular electrostatic potential

Electrostatic potential maps are very useful three dimensional diagrams used to visualize the charge distributions and charge related properties of molecules. The MEP is typically visualized through mapping its values onto the surface reflecting the molecules boundaries so it allows us to visualize the size and shape of molecules. This can be generated by overlapping the vdW radii of all atoms in the molecule. MEP diagram has been also used to predict the reactive sites for electrophilic and nucleophilic attack, and in studies of biological recognition and hydrogen bonding interactions [47, 48].The MEP of the studied compounds calculated using B3LYP method with 6–311G(d,p) basis set is shown in Fig. 4. This figure provides a visual representation of the chemically active sites and comparative reactivity of atoms. Potential increases in the order red < orange < yellow < green < blue. For all the studied compounds, the negative regions (red) are mainly localized over the carbonyl oxygen atoms (–0.0271 to –0.0409 au). The maximum positive regions (blue) are localized on the phenyl ring attached to the N-atom of the quinazoline ring in case of

2 and at the carbonyl carbon for **14**. We noted that, the presence of halogen group attached to the phenyl ring shifts its electrostatic potential to more positive value for compounds **2**. Also, the negative MEP values at the fused phenyl ring of the quinazoline moiety are decreased, hence the ring become deactivated towards electrophilic attack.

NLO properties

The development of materials with large nonlinear optical (NLO) properties has been of great interest in past few decades. These materials find numerous device applications, from lasers to optical switches and electronics [49]. So far, the organic π-conjugated molecules have been considered mostly for this purpose because of their easy functionalization to fine tune the desired properties and the ease of fabrication and integration into devices [50-52]. NLO is very important in areas such as telecommunications, optical interconnections and signal processing [53, 54].

The components of the static polarizability components (α_0) and the average polarizability (α_0) of the studied compound are given in Table 5. The α_0 values are calculated to be in the order **2c>2b>2a>14c >14a**. The ranking of the HOMO-LUMO energy gap is in the opposite order. It is well known that compounds having good NLO activity are characterized by high value of polarizability and low energy gap. It could be seen from the presence investigation that **2c** has the highest polarizability and lowest energy gap; hence **2c** could be the best candidates for NLO applications.

NMR spectra

The isotropic magnetic shielding (IMS) values calculated using the GIAO approach at the 6-311G(d,p) level are used to predict the ^{13}C and ^{1}H chemical shifts (δ_{calc}) for the studied compounds and the results are correlated to the experimental NMR data (δ_{exp}) in $CDCl_3$ solvent. The experimental and theoretical ^{1}H- and ^{13}C-NMR chemical shift values of the studied compounds are given in Table S4 (Supplementary Information). According to these results, the calculated chemical shifts are in compliance with the experimental findings. A representative example for the correlation between the experimental and theoretical chemical shifts of the studied is shown in Fig. 5. It can be seen that, there is good agreement between the experimental and the calculated chemical shifts. The correlation coefficients for the carbon–13 (R^2 = 0.970) and proton (R^2 = 0.976) are high for **2a**.

Conclusion

The molecular structure, electronic and spectroscopic properties of newly synthesized S-alkylated products of the 3-aryl-2-mercapto-3H-quinazolin-4-one; **1** and N-alkylated products of 3-aryl-1*H*,3*H*-quinazolin-2,4-dione; **12** were investigated using B3LYP/6-311G(d,p) method. The structures of the products were experimentally identified using m.p., IR and ^{1}HNMR data. The synthesized compounds were prepared in good yields via efficient nucleophilic substitution reaction of SH and NH substrates. The chemical reactivity descriptors that could help to understand the biological activity of the products are also predicted. The reactivity of these substrates toward the nucleophilic attack at either the N or S/O sites was predicted using the reactivity descriptors obtained from the DFT calculations. DFT reactivity studies showed that **12** have the N-site with the highest nucleophilicity while the S-site is the most nucleophilic in **1**.

References :

1. J. H. Chan,; J. S. Hong,; L. F. Kuyper,; M. L. Jones,; D. P. Baccanari,; R. L.Tansik,; C. M.Boytos,; S. K.Rudolph,; A. D. Brown, J. Heterocycl. Chem. 1997, 34, 145.
2. S. L. Gackenheimer,; J. M. Schaus,; D. R. Gehlert, J. Pharmacol. Exp. Ther. 113 (1996) 732.
3. R. O. Dempcy,; Skibo, E. B. Biochemistry 30 (1991) 8480.
4. Nordisk-Droge. 18113; Patent, N. A. Ed.; Nordisk Drogeand Kemi-Kalieforretning AIS: Netherlands, 1965.
5. D. J. Connolly,; D. Cusack,; T. P. O'Sullivan; P. J. Guiry Tetrahedron 61 (2005) 10153.
6. D. W. Fry,; A. J. Kraker,; A. McMichael,; L. A. Ambroso,; J. M. Nelson,; W. R. Leopold,; R. W. Connors,; A. J. Bridges, Science 265 (1994) 1093.
7. T. M. Traxler,; P. Furet,; H. Melt,; E. Buchdunger,; T. Meyer,; N. Lydon, J. Med. Chem. 39 (1996) 2289.
8. J. B. Hynes,; A. Tomazić,; A. Kumar,; V. Kumar,; J. H. Freisheim, J. Heterocycl. Chem. 28 (1991) 1981
9. A. Witt,; J. Bergman, Curr. Org. Chem. 7 (2003) 659.
10. (a) W. L. F. Armarego, Adv. Heterocycl. Chem. 24 (1979) 1; (b) S. Johne, Prog. Chem. Org. Nat. Prod. 46 (1984) 159; (c) Johne, S. Rodd's Chemistry of Carbon Compounds (supplements to the 2nd ed.); M. F. Ansell, , Ed.; Elsevier: Amsterdam 1995; Vol. IV I/J, 223–240; (d) D. J. Brown, Quinazolines. In The Chemistry of Heterocyclic Compounds (supplement I); Wiley: New York, NY, 1996, 55. (e) A. L. D'yakonov,; M. Telezhenetskaya, V. Chem. Nat. Compd. 33 (1997) 221; (f) Johne, S. Rodd's Chemistry of Carbon Compounds (second supplements to the 2nd ed.); M.Sainsbury, Ed.; Elsevier: Amsterdam 2000; IV I/J, 203–231; (g) S. R. Padala,; P. R. Padi,; V. Thipireddy, Heterocycles 60 (2003) 183; (h) D. J. Connolly,; D.Cusack,; T. P. O'Sullivan,; P. J. Guiry, Tetrahedron 61 (2005) 10153; (i) Z. Ma, Y. Hano, T. Nomura, Heterocycles, 65 (2005) 2203. (j) V. S. Patil, V. S. Padalkar, N. Sekar, J. fluoresce. 24 (2014) 1077-1086, (k) H. S. Bhatti, S. Seshadri, Coloration Technology 120 (2006) 101 – 107.

11. M. F. Grundon, Nat. Prod. Rep. 1 (1984) 195; (ii) M. F. Grundon, Nat. Prod. Rep. 2 (1985) 393; (iii) M. F. Grundon, Nat. Prod. Rep. 4 (1987) 225; (iv) M. F. Grundon, Nat. Prod. Rep. 5 (1988) 293; (v) M. F. Grundon, Nat. Prod. Rep. 7 (1990) 131; (vi) M. F. Grundon, Nat. Prod. Rep., 8 (1991) 53; (b) (i) J. P. Michael, Nat. Prod. Rep. 9 (1992) 25; (ii) J. P. Michael, Nat. Prod. Rep. 10 (1993) 99; (iii) J. P. Michael, Nat. Prod. Rep. 11 (1994) 163; (iv) J. P. Michael, Nat. Prod. Rep. 12 (1995) 77; (v) J. P. Michael, Nat. Prod. Rep. 12 (1995) 465; (vi) J. P. Michael, Nat. Prod. Rep., 14 (1997) 11; (vii) J. P. Michael, Nat. Prod. Rep. 14 (1997) 605; (viii) J. P. Michael, Nat. Prod. Rep. 15 (1998) 595; (ix) J. P. Michael, Nat. Prod. Rep. 16 (1999) 697; (x) J. P. Michael, Nat. Prod. Rep. 17 (2000) 603; (xi) J. P. Michael, Nat. Prod. Rep. 18 (2001) 543; (xii) J. P. Michael, Nat. Prod. Rep. 19 (2002) 742; (xiii) J. P. Michael, Nat. Prod. Rep., 20 (2003) 476; (xiv) J. P. Michael, Nat. Prod. Rep. 21 (2004) 650; (xv) J. P. Michael, Nat. Prod. Rep. 22 (2005) 627.
12. S. B. Mhaske,; N. P. Argade Tetrahedron 62 (2006) 9787.
13. A. M. Alafeefy J. Saudi Chem. Soc. 15 (2011) 337.
14. V. V. Orisik; Y. L. Zborovs'kii; A. A. Dobosh; V. I. Staninets; S. M. Khripak, Ukrainskii Khimicheskii Zhurnal 68 (2002) 36.
15. Y. A. Azey, Chem. Heterocycl. Compd., 43 (2007) 356.
16. M. J. Frisch, et al., Gaussian–03, Revision C.01, Gaussian, Inc., Wallingford, CT, (2004).
17. GaussView, Version 4.1, R. Dennington II, T. Keith, J. Millam, Semichem Inc., Shawnee Mission, KS, (2007).
18. G.A. Zhurko, D.A. Zhurko, Chemcraft: Lite Version Build 08 (Freeware), 2005.
19. A. D. Becke, Phys. Rev. A 38 (1988) 3098-3100.
20. W. Wang, W.J. Mortier, J. Am. Chem. Soc. 108 (1986) 5708-5711.
21. E.D. Glendening, A.E. Reed, J.E. Carpenter, F. Weinhold, NBO Version 3.1, CI,University of Wisconsin, Madison, (1998).
22. D.R. Roy, R. Parthasarathi, J. Padmanabhan, U. Sarkar, V. Subramanium, P.K. Chattaraj J. Phys. Chem. A 110 (2006) 1084–1093.
23. W. Yang, W.J. Mortier J. Am. Chem. Soc. 108 (1986) 5708–5711.
24. P. Perez, L.R. Domingo, M. Doque-Norena, E. Chamorro J. Mol. Struct.: (THEOCHEM) 895 (2009) 86–91.
25. V. J. P.Mishra; S. Kashaw; J. P. Stables Eur. J. Med. Chem. 43 (2008).

26. F. A. M. Al-Omary, L. A. Abou-zeid, M. N. Nagi, E. E. Habib, A. A.-M. Abdel-Aziz, A. S. El-Azab, S. G. Abdel-Hamide, M. A. Al-Omar, A. M. Al-Obaid, H. I. El-Subbagh, Bioorg. Med. Chem. 18 (2010) 2849.
27. A. S., El-Azab Phosphorus, Sulfur, and Silicon 182 (2007) 333.
28. M.Belkadi; A. A., Othman Arkivoc (2006) 183.
29. V. Pilepicć, S. Uršić, Nucleophilic reactivity of the nitroso group. Fukui function DFT calculations for nitrosobenzene and 2-methyl-2-nitrosopropane, J. Mol. Struct. (Theochem) 538 (2001) 41-49 and reference within.
30. H. Chermette, Chemical reactivity indexes in density functional theory, J. Comput. Chem. 20 (1999) 129-154.
31. R. K. Roy, F. De Proft, P. Geerlings J. Phys. Chem. A 102 (1998) 7035-7040.
32. W. Langenaeker, F. De Proft, P. Geerlings J. Mol. Struct. (Theochem) 362 (1996) 175-179.
33. F. Al-Omran, R. M. Mohareb and A. A. El-Khair, Molecules 16 (2011) 6129-6147.
34. Y Kitano, M. Kashiwag, Y. Kinoshita, Acta Cryst. (1972). B28, 1223-1231.
35. I. Sidir, Y.G. Sidir, M. Kumalar, E. Tasal, J. Mol. Struct. 964 (2010) 134-151.
36. K. Fukui, T. Yonezawa, H.J. Shingu J. Chem. Phys. 20 (1952) 722–725.
37. N. Sinha, O. Prasad, V. Narayan, S.R. Shukla, J. Mol. Simul. 37 (2011) 153–163.
38. L. Padmaja, C. Ravikumar, D. Sajan, I. H. Joe, V. S. Jayakumar, G. R. Pettit, F. O. Neilsen, J. Raman Spectrosc. 40 (2009) 419–428.
39. C. Ravikumar, I. H. Joe, V. S. Jayakumar, Chem. Phys. Lett. 460 (2008) 552–558.
40. R.G. Pearson, J. Org. Chem. 54 (1989) 1430–1432.
41. R.G. Parr, R.G. Pearson, J. Am. Chem. Soc. 105 (1983) 7512–7516.
42. P. Geerlings, F. De Proft, W. Langenaeker, Chem. Rev. 103 (2003) 1793–1873.
43. R.G. Parr, L. Szentpaly, S. Liu, J. Am. Chem. Soc. 121 (1999) 1922–1924.
44. K. Chattaraj, S. Giri, J. Phys. Chem. A 111 (2007) 11116–11121.
45. R.G. Parr, W. Yang, Density-Functional Theory of Atoms and Molecules, Oxford University Press, New York, 1989.

46. R. N. Singh, A. Kumar, R. K. Tiwari, P. Rawat, V. P. Gupta, J. Mol. Struct. 1035 (2013) 427–440.
47. E. Scrocco, J. Tomasi, in: P. Lowdin (Ed.), Advances in Quantum Chemistry, vol. 2, Academic Press, New York, 1978.
48. J.S. Murray, K. Sen, Molecular Electrostatic Potentials, Concepts and Applications, Elsevier, Amsterdam, 1996.
49. P. N. Prasad, D. J. Williams, Introduction to nonlinear optical effects in molecules and polymers, (New York: Wiley) 1991.
50. G. A. Lindsay, K. D. Singer, Polymers for second-order nonlinear optics, ACS Symposium Series, No. 601 (Washington, DC: ACS) 1995.
51. D. Burland Chem. Rev. 94 (1994) 1-2.
52. E. Hanamura Phys. Rev. B37 (1988) 1273-1244.
53. V. M. Geskin, C. Lambert, J. L. Bredas, J. Am. Chem. Soc. 125 (2003) 15651-15658.
54. D. Sajan, H. Joe, V.S. Jayakumar, J. Zaleski, J. Mol. Struct. 785 (2006) 43-53.

Table 1 The calculated quantum chemical parameters of the studied reactants.

Compound	E_{HOMO}	E_{LUMO}	ΔE	N
		Gas		
1a	-6.0584	-1.8825	4.1759	3.310
1b	-6.1993	-2.0074	4.1919	3.169
1c	-6.1906	-2.0039	4.1868	3.177
12a	-6.6407	-1.6615	4.9792	2.727
12b	-6.7781	-1.8126	4.9656	2.590
12c	-6.7683	-1.8139	4.9544	2.600
		Solution		
1a	-6.2946	-1.8014	4.4932	2.623
1b	-6.3419	-1.8300	4.5120	2.576
1c	-6.3384	-1.8289	4.5095	2.579
12a	-6.5019	-1.5853	4.9166	2.416
12b	-6.5275	-1.6218	4.9057	2.390
12c	-6.5286	-1.6164	4.9122	2.389

Table 2 The reactivity descriptors of the studied reactants.

Compound	Q_N	Q_{N-1}	f_k^-	N_k	Q_N	Q_{N-1}	f_k^-	N_k
	Gas (N-site)				Gas (S-site)			
1a	-0.5645	-0.5276	0.0369	0.1221	-0.1861	0.2886	0.4746	1.5709
1b	-0.5638	-0.5297	0.0341	0.1080	-0.1823	0.2448	0.4272	1.3536
1c	-0.5638	-0.5289	0.0349	0.1108	-0.1821	0.2131	0.3952	1.2559
	Solution (N-site)				Solution (S-site)			
1a	-0.5554	-0.5227	0.0328	0.0860	-0.3219	0.3594	0.6813	1.7869
1b	-0.5544	-0.5217	0.0327	0.0841	-0.3166	0.3508	0.6674	1.7188
1c	-0.5544	-0.5210	0.0334	0.0861	-0.3170	0.3363	0.6534	1.6851
	Gas (N-site)				Gas (O-site)			
12a	-0.6028	-0.4954	0.1074	0.2930	-0.6107	-0.5160	0.0947	0.2583
12b	-0.6018	-0.5122	0.0896	0.2320	-0.6107	-0.5469	0.0639	0.1654
12c	-0.6017	-0.5210	0.0807	0.2098	-0.6108	-0.5546	0.0562	0.1460
	Solution (N-site)				Solution (O-site)			
12a	-0.6002	-0.4507	0.1495	0.3611	-0.6700	-0.5528	0.1172	0.2831
12b	-0.5996	-0.4503	0.1492	0.3567	-0.6679	-0.5512	0.1166	0.2788
12c	-0.5996	-0.4488	0.1508	0.3602	-0.6682	-0.5530	0.1152	0.2753

Table 3 The calculated geometric parameters of the studied compounds (**2a-c**, **14a** and **14c**) using the B3LYP/6-311G(d,p) method.

Parameter	Calc.			Exp.[33]	Parameter	Calc.		Exp.[34]
	2a	**2b**	**2c**			**14a**	**14c**	
R(1-2)	1.404	1.405	1.405	1.388	R(1-2)	1.397	1.397	1.415
R(1-6)	1.383	1.383	1.383	1.366	R(1-6)	1.384	1.384	1.386
R(1-19)	1.084	1.084	1.084		R(1-18)	1.083	1.083	
R(2-3)	1.383	1.383	1.383	1.382	R(2-3)	1.388	1.388	1.378
R(2-20)	1.084	1.084	1.084		R(2-19)	1.084	1.084	
R(3-4)	1.407	1.406	1.406	1.404	R(3-4)	1.405	1.405	1.402
R(3-21)	1.083	1.083	1.083		R(3-20)	1.079	1.079	
R(4-5)	1.409	1.406	1.406	1.397	R(4-5)	1.406	1.406	1.392
R(4-7)	1.384	1.384	1.384	1.389	R(4-7)	1.398	1.398	1.379
R(5-6)	1.402	1.402	1.402	1.398	R(5-6)	1.399	1.399	1.391
R(5-10)	1.465	1.463	1.463	1.456	R(5-10)	1.472	1.471	1.478
R(6-22)	1.083	1.083	1.083		R(6-21)	1.083	1.083	
R(7-8)	1.287	1.286	1.286	1.285	R(7-8)	1.395	1.393	1.372
R(8-9)	1.389	1.398	1.398	1.400	R(7-28)	1.476	1.476	
R(8-12)	1.788	1.799	1.799	1.761	R(8-9)	1.403	1.405	1.414
R(9-10)	1.425	1.431	1.431	1.402	R(8-27)	1.214	1.214	1.201
R(9-13)	1.446	1.444	1.444	1.440	R(9-10)	1.409	1.410	1.383
R(10-11)	1.214	1.214	1.214	1.219	R(9-12)	1.449	1.446	1.455
R(12-28)	1.849	1.856	1.856		R(10-11)	1.213	1.213	1.213
R(13-14)	1.392	1.393	1.393	1.382	R(12-13)	1.390	1.390	1.396
R(13-18)	1.392	1.393	1.393	1.378	R(12-17)	1.390	1.390	1.391
R(14-15)	1.392	1.391	1.392	1.384	R(13-14)	1.392	1.391	1.423
R(14-23)	1.083	1.082	1.082		R(13-22)	1.083	1.083	
R(15-16)	1.393	1.391	1.391	1.355	R(14-15)	1.393	1.391	1.384
R(15-24)	1.084	1.082	1.082		R(14-23)	1.084	1.082	
R(16-17)	1.394	1.391	1.391	1.373	R(15-16)	1.393	1.391	1.384
R(16-25)	1.084	1.758	1.916		R(15-24)	1.084	1.917	
R(17-18)	1.391	1.391	1.391	1.393	R(16-17)	1.392	1.391	1.399
R(17-26)	1.084	1.082	1.082		R(16-25)	1.084	1.082	
R(18-27)	1.083	1.082	1.083		R(17-26)	1.083	1.083	
R(28-29)	1.093	1.094	1.094		R(28-29)	1.092	1.092	
R(28-30)	1.088	1.090	1.090		R(28-30)	1.090	1.090	
R(28-31)	1.497	1.494	1.495		R(28-31)	1.505	1.505	
R(31-32)	1.087	1.087	1.087		R(31-32)	1.087	1.087	
R(31-33)	1.329	1.330	1.330		R(31-33)	1.329	1.329	
R(33-34)	1.084	1.084	1.084		R(33-34)	1.087	1.086	
R(33-35)	1.084	1.085	1.086		R(33-35)	1.084	1.084	
A(2-1-6)	119.8	120.0	120.0	119.9	A(2-1-6)	119.0	119.0	119.4
A(2-1-19)	120.0	119.9	119.9		A(2-1-18)	120.5	120.5	
A(1-2-3)	120.8	120.7	120.7	120.9	A(1-2-3)	121.3	121.3	120.7
A(1-2-20)	119.6	119.6	119.6		A(1-2-19)	119.9	119.9	
A(6-1-19)	120.2	120.1	120.1		A(6-1-18)	120.6	120.5	
A(1-6-5)	120.0	119.8	119.8	120.4	A(1-6-5)	120.6	120.6	120.1
A(1-6-22)	121.8	121.8	121.8		A(1-6-21)	121.9	121.9	
A(3-2-20)	119.6	119.7	119.7		A(3-2-19)	118.8	118.8	
A(2-3-4)	120.2	119.9	120.0	119.8	A(2-3-4)	120.1	120.1	119.2
A(2-3-21)	121.5	121.9	121.9		A(2-3-20)	119.3	119.3	
A(4-3-21)	118.3	118.1	118.1		A(4-3-20)	120.6	120.6	
A(3-4-5)	118.8	119.2	119.2	118.9	A(3-4-5)	118.6	118.6	120.3
A(3-4-7)	119.2	118.8	118.8	118.6	A(3-4-7)	122.0	121.9	119.8
A(5-4-7)	122.0	122.0	122.0	122.5	A(5-4-7)	119.4	119.5	119.9
A(4-5-6)	120.5	120.4	120.4	120.2	A(4-5-6)	120.5	120.5	120.2
A(4-5-10)	119.6	119.6	119.6		A(4-5-10)	120.8	120.9	119.4
A(4-7-8)	118.5	119.0	119.0	117.3	A(4-7-8)	123.0	123.0	124.6

A(6-5-10)	119.9	120.0	120.0	119.9	A(4-7-28)	121.3	121.3	
A(5-6-22)	118.3	118.4	118.4		A(6-5-10)	118.7	118.7	120.4
A(5-10-9)	113.8	114.0	114.0	114.0	A(5-6-21)	117.4	117.5	
A(5-10-11)	125.7	125.2	125.2	126.0	A(5-10-9)	114.7	114.6	115.4
A(7-8-9)	124.6	124.2	124.1	124.8	A(5-10-11)	124.2	124.3	123.6
A(7-8-12)	120.7	115.9	115.9	122.0	A(8-7-28)	115.7	115.7	
A(9-8-12)	114.8	119.9	119.9	113.2	A(7-8-9)	116.4	116.4	115.2
A(8-9-10)	121.5	121.1	121.1	121.5	A(7-8-27)	122.1	122.3	121.6
A(8-9-13)	121.5	123.0	122.9	120.2	A(7-28-29)	108.8	108.8	
A(8-12-28)	100.4	102.9	103.0		A(7-28-30)	105.5	105.5	
A(10-9-13)	117.0	115.8	115.9	118.3	A(7-28-31)	113.5	113.4	
A(9-10-11)	120.6	120.8	120.8	120.0	A(9-8-27)	121.5	121.3	122.9
A(9-13-14)	119.5	119.9	119.9	95.7	A(8-9-10)	125.7	125.7	125.4
A(9-13-18)	119.7	120.0	120.0	119.6	A(8-9-12)	116.7	116.6	116.5
A(12-28-29)	103.0	101.3	101.3		A(10-9-12)	117.7	117.7	118.1
A(12-28-30)	107.4	110.3	110.3		A(9-10-11)	121.2	121.0	121.0
A(12-28-31)	112.7	113.2	113.2		A(9-12-13)	119.7	119.9	117.9
A(14-13-18)	120.8	120.0	120.0	121.5	A(9-12-17)	119.6	119.7	119.0
A(13-14-15)	119.5	120.2	120.2	118.6	A(13-12-17)	120.7	120.4	123.1
A(13-14-23)	119.6	119.7	119.8		A(12-13-14)	119.6	120.1	116.8
A(13-18-17)	119.5	120.2	120.2	118.6	A(12-13-22)	119.6	119.9	
A(13-18-27)	119.6	119.9	119.9		A(12-17-16)	119.5	120.1	118.4
A(15-14-23)	120.9	120.1	120.0		A(12-17-26)	119.7	119.9	
A(14-15-16)	120.1	119.2	119.2	120.5	A(14-13-22)	120.8	120.1	
A(14-15-24)	119.7	120.6	120.4		A(13-14-15)	120.1	119.1	121.2
A(16-15-24)	120.2	120.2	120.5		A(13-14-23)	119.7	120.5	
A(15-16-17)	120.1	121.2	121.2	121.2	A(15-14-23)	120.2	120.5	
A(15-16-25)	120.0	119.4	119.4		A(14-15-16)	120.0	121.3	120.0
A(17-16-25)	120.0	119.4	119.4		A(14-15-24)	120.0	119.4	
A(16-17-18)	120.1	119.2	119.2	119.7	A(16-15-24)	120.0	119.3	
A(16-17-26)	120.2	120.2	120.5		A(15-16-17)	120.1	119.1	120.4
A(18-17-26)	119.7	120.6	120.3		A(15-16-25)	120.2	120.5	
A(17-18-27)	120.9	119.9	119.9		A(17-16-25)	119.7	120.5	
A(29-28-30)	109.5	108.1	108.2		A(16-17-26)	120.8	120.1	
A(29-28-31)	111.5	111.1	111.1		A(29-28-30)	108.2	108.1	
A(30-28-31)	112.2	112.2	112.2		A(29-28-31)	111.4	111.5	
A(28-31-32)	116.0	116.0	116.0		A(30-28-31)	109.2	109.2	
A(28-31-33)	124.2	124.0	124.0		A(28-31-32)	115.2	115.2	
A(32-31-33)	119.8	120.1	120.1		A(28-31-33)	124.5	124.5	
A(31-33-34)	121.4	121.5	121.5		A(32-31-33)	120.2	120.2	
A(31-33-35)	121.5	121.7	121.7		A(31-33-34)	121.8	121.8	
A(34-33-35)	117.2	116.8	116.8		A(31-33-35)	121.6	121.6	
					A(34-33-35)	116.6	116.6	

Table 4 The calculated natural atomic charges of the studied compounds (**2a-c**, **14a** and **14c**) using the B3LYP/6-311G(d,p) method.

Atom	**2a**	**2b**	**2c**	**Atom**	**14a**	**14c**
C1	-0.2091	-0.1988	-0.1989	C1	-0.2213	-0.2201
C2	-0.1703	-0.1712	-0.1712	C2	-0.1536	-0.1522
C3	-0.1995	-0.1871	-0.1871	C3	-0.2455	-0.2447
C4	0.1876	0.1750	0.1751	C4	0.2092	0.2093
C5	-0.1797	-0.1710	-0.1711	C5	-0.1799	-0.1811
C6	-0.1441	-0.1465	-0.1464	C6	-0.1308	-0.1300
N7	-0.5683	-0.5069	-0.5070	N7	-0.4598	-0.4590
C8	0.3672	0.3529	0.3526	C8	0.8486	0.8483
N9	-0.5017	-0.5031	-0.5032	N9	-0.5190	-0.5199
C10	0.6919	0.6914	0.6916	C10	0.6958	0.6960
O11	-0.5943	-0.5960	-0.5960	O11	-0.5869	-0.5864
S12	0.2530	0.2230	0.2239	C12	0.1667	0.1649
C13	0.1386	0.1486	0.1499	C13	-0.1846	-0.1667
C14	-0.1856	-0.1779	-0.1784	C14	-0.1880	-0.2179
C15	-0.1885	-0.2227	-0.2226	C15	-0.1922	-0.0752
C16	-0.1861	-0.0106	-0.0758	C16	-0.1879	-0.2178
C17	-0.1880	-0.2207	-0.2207	C17	-0.1852	-0.1675
C18	-0.1804	-0.1717	-0.1730	H18	0.2074	0.2082
H19	0.2046	0.2059	0.2059	H19	0.2044	0.2052
H20	0.2031	0.2052	0.2052	H20	0.2147	0.2154
H21	0.2114	0.2181	0.2181	H21	0.2281	0.2285
H22	0.2238	0.2249	0.2249	H22	0.2098	0.2157
H23	0.2151	0.2230	0.2233	H23	0.2032	0.2209
H24	0.2055	0.2223	0.2226	H24	0.2020	0.0552[b]
H25	0.2037	-0.0030[a]	0.0612[b]	H25	0.2032	0.2209
H26	0.2054	0.2226	0.2229	H26	0.2098	0.2159
H27	0.2151	0.2210	0.2210	O27	-0.6247	-0.6247
C28	-0.5038	-0.5008	-0.5011	C28	-0.2108	-0.2107
H29	0.2185	0.2253	0.2253	H29	0.1969	0.1976
H30	0.2375	0.2120	0.2124	H30	0.2449	0.2452
C31	-0.1994	-0.1969	-0.1969	C31	-0.1807	-0.1820
H32	0.1897	0.1997	0.1996	H32	0.1988	0.1988
C33	-0.3462	-0.3571	-0.3571	C33	-0.3641	-0.3626
H34	0.1868	0.1928	0.1927	H34	0.1781	0.1784
H35	0.1866	0.1782	0.1783	H35	0.1933	0.1939

[a]Cl [b]Br

Table 5 The dipole moments components μ (D), polarizability components (a.u.) and the average polarizability α_0 of the studied compounds.

Parameter	2a	2b	2c	14a	14c
μ_x	0.048	1.353	1.285	3.180	-5.267
μ_y	2.132	1.380	1.252	-0.666	0.703
μ_z	-0.215	0.594	0.578	-0.200	-0.177
μ	2.1438	2.0218	1.8848	3.2555	5.3171
α_{xx}	309.146	341.321	354.458	280.111	333.474
α_{xy}	7.374	-10.354	-19.983	8.181	6.630
α_{yy}	218.591	192.251	197.730	188.959	194.517
α_{xz}	-5.240	-2.272	-4.388	-0.499	-1.001
α_{yz}	-2.834	-18.986	-19.079	2.072	-5.168
α_{zz}	146.218	180.215	183.689	136.071	142.406
α_0	224.652	237.929	**245.292**	201.714	223.466

Table 6 The calculated chemical potential (μ), electronegativity (χ), global hardness (η), softness (S) and global electrophilicity index (ω) (in eV) for the studied compound.

Descriptor	2a	2b	2c	14a	14c
I	6.1602	6.4652	6.4554	6.5017	6.6260
A	1.3394	1.7271	1.7285	1.5723	1.7037
χ	3.7498	4.0962	4.0919	4.0370	4.1649
μ	-3.7498	-4.0962	-4.0919	-4.0370	-4.1649
η	2.4104	2.3690	2.3635	2.4647	2.4612
s	0.2074	0.2111	0.2116	0.2029	0.2032
ω	2.9167	3.5412	3.5423	3.3061	3.5240

Table 7 The most important electronic transition bands calculated using the TD-DFT method for the studied compounds.

		2a
295.4	0.0559	H→L (87%)
273.0	0.1968	H→L+1 (75%)
217.9	0.1669	H-5→L+1 (25%), H-4→L+1 (37%)
216.0	0.1903	H-5→L+2 (18%), H-3→L (23%), H-2→L+2 (10%)
		2b
311.6	0.0609	H-1→L (17%), H→L (69%)
280.4	0.2085	H-1→L (51%), H→L+1 (25%)
222.2	0.2648	H-7→L (11%), H-3→L+1 (26%), H-1→L+4 (24%)
218.8	0.2171	H-3→L+1 (15%), H-1→L+4 (46%)
		2c
311.8	0.0629	H-1→L (15%), H→L (70%)
281.2	0.2217	H-1→L (51%), H→L+1 (28%)
222.7	0.1765	H-7→L (18%), H-6→L (10%), H-4→L+2 (12%), H-3→L+1 (11%), H-2→L+3 (13%)
219.4	0.2112	H-3→L+1 (11%), H-2→L+2 (13%), H-1→L+5 (46%)
		14a
289.1	0.0701	H→L (85%)
214.2	0.4694	H-7→L (21%), H-4→L (21%), H→L+1 (16%)
210.6	0.2037	H-7→L (19%), H-2→L+1 (45%)
192.1	0.0875	H-8→L (12%), H-7→L+1 (16%), H-6→L+1 (26%), H→L+5 (13%)
180.4	0.1632	H-2→L+5 (55%)
		14c
289.6	0.0736	H→L (85%)
221.3	0.4203	H-6→L (10%), H-1→L+2 (57%)
212.9	0.1044	H-8→L (48%), H-3→L+1 (12%)
211.1	0.2767	H-8→L (31%), H-5→L (10%)
204.8	0.1063	H-10→L (16%), H-4→L+1 (32%), H-2→L+1 (10%), H→L+6 (14%)

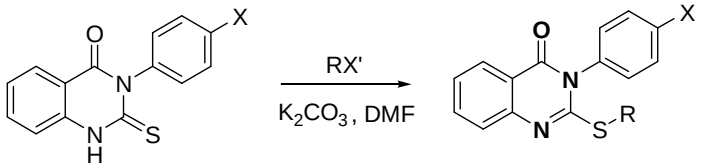

1a: X=H
1b: X=Cl
1c: X=Br

2a: X=H, R= $CH_2CH{=}CH_2$
2b: X=Cl, R= $CH_2CH{=}CH_2$
2c: X=Br, R= $CH_2CH{=}CH_2$
3a: X=H, R= CH_2COPh
3b: X=Cl, R= CH_2COPh
3c: X=Br, R= CH_2COPh
4a: X=H, R= $CH_2CH_2CH_2OH$
4b: X=Cl, R= $CH_2CH_2CH_2OH$
4c: X=Br, R= $CH_2CH_2CH_2OH$
5a: X=H, R= CH_2COOEt
5b: X=Cl, R= CH_2COOEt
5c: X=Br, R= CH_2COOEt

Scheme 1

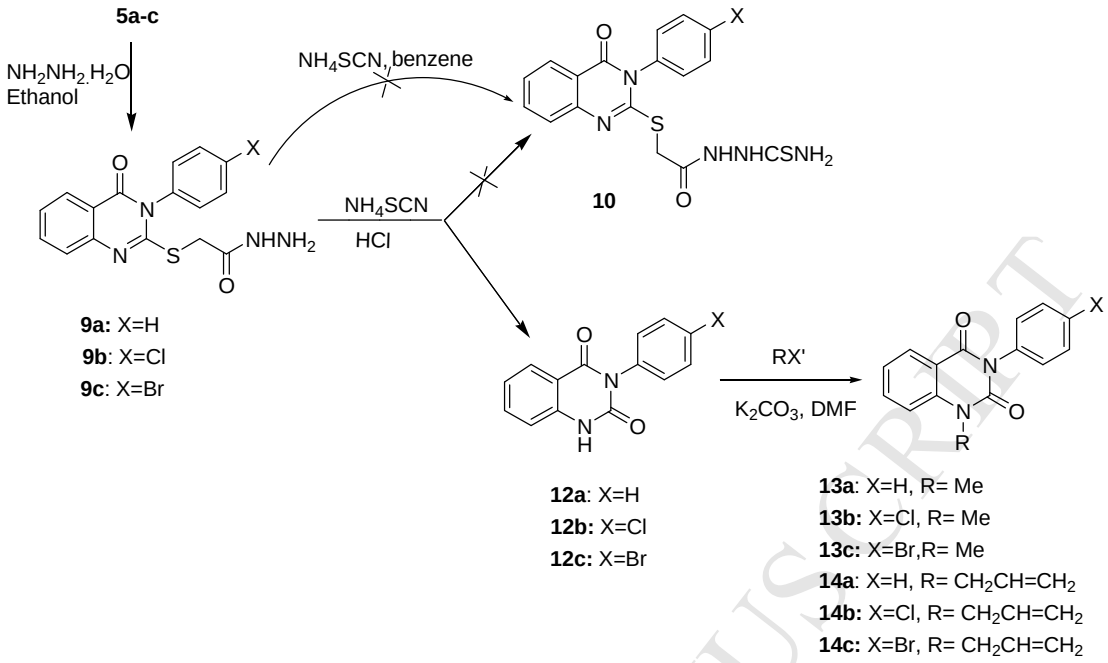

Scheme 2

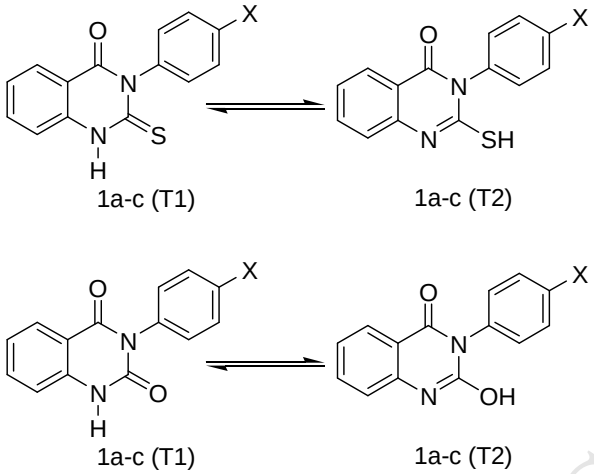

Scheme 3

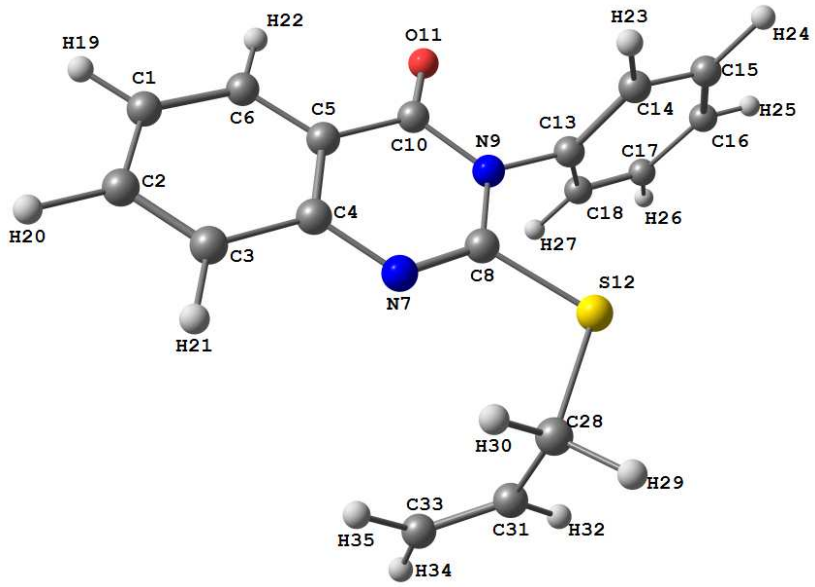

2a

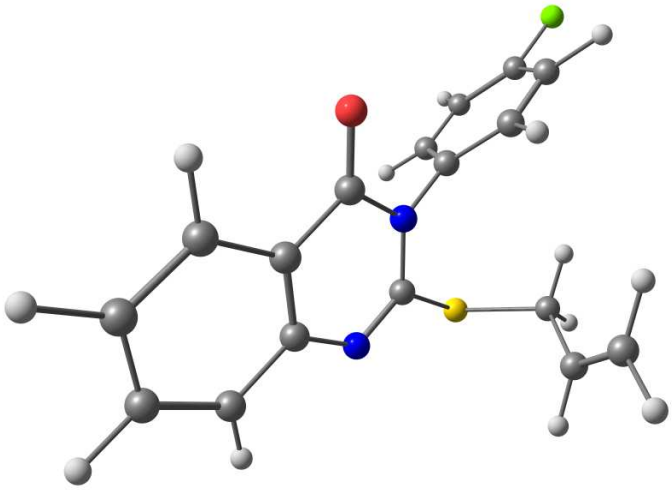

2b

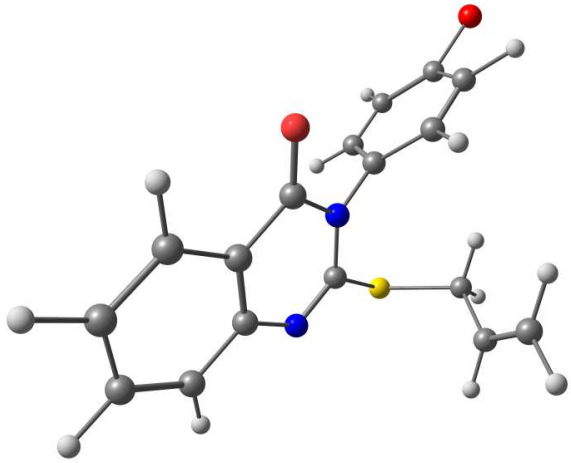

2c

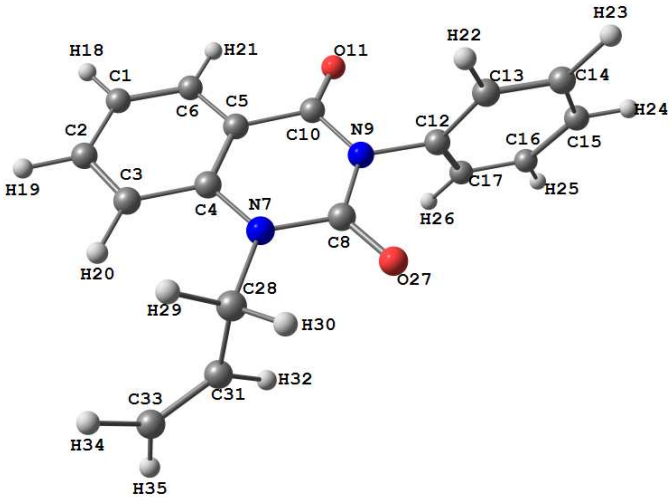

14a

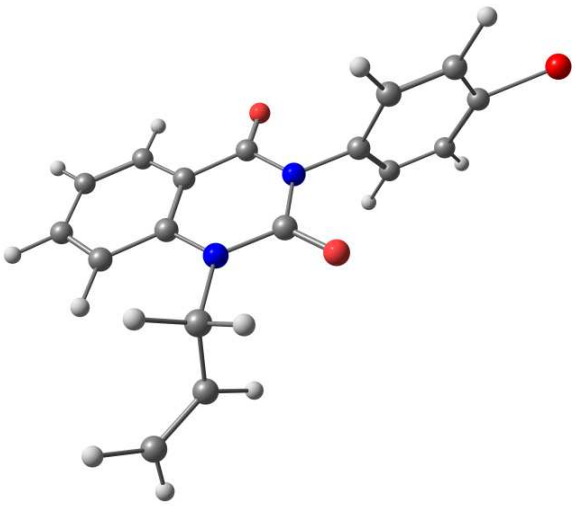

14c

Fig. 1 The optimized molecular structures of the studied compounds (**2a-c**, **14a** and **14c**) calculated using B3LYP/6-311G(d,p) method.

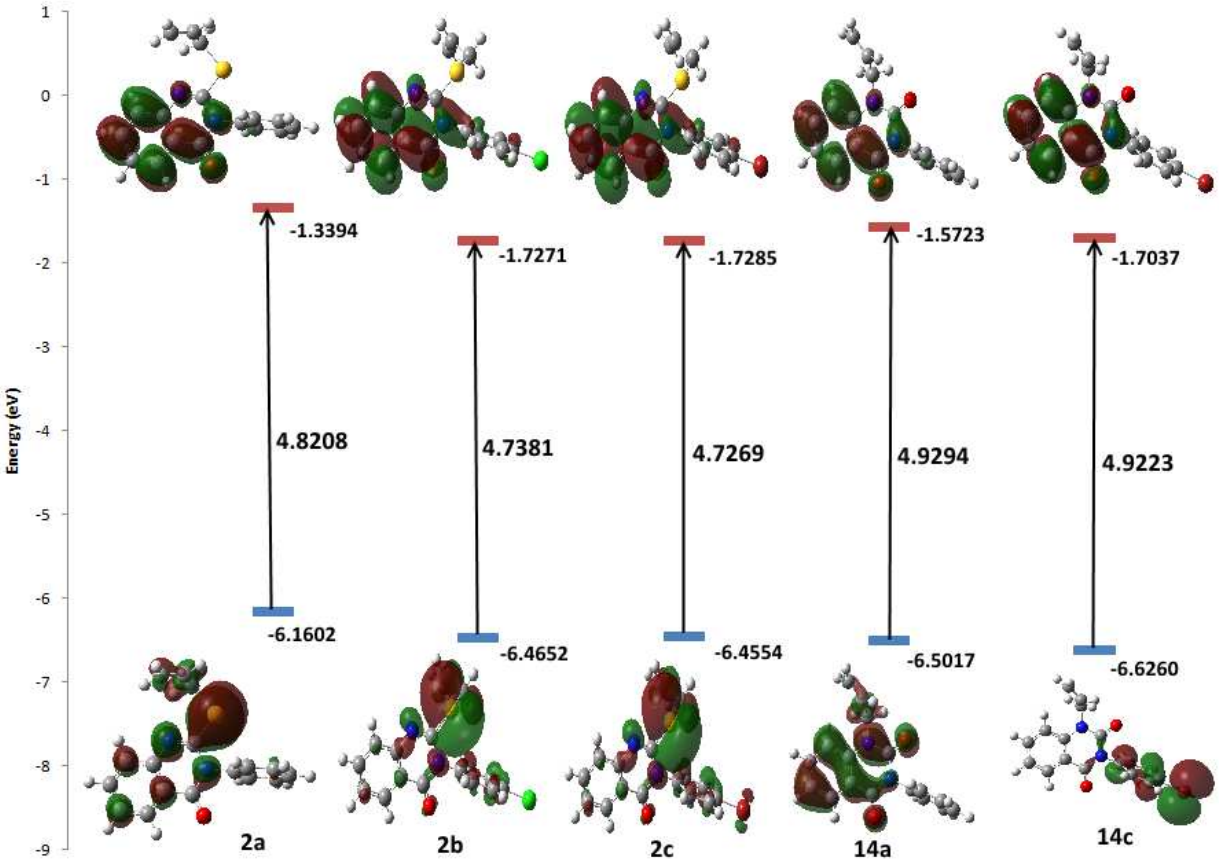

Fig. 2 The ground state isodensity surface plots for the frontier molecular orbitals.

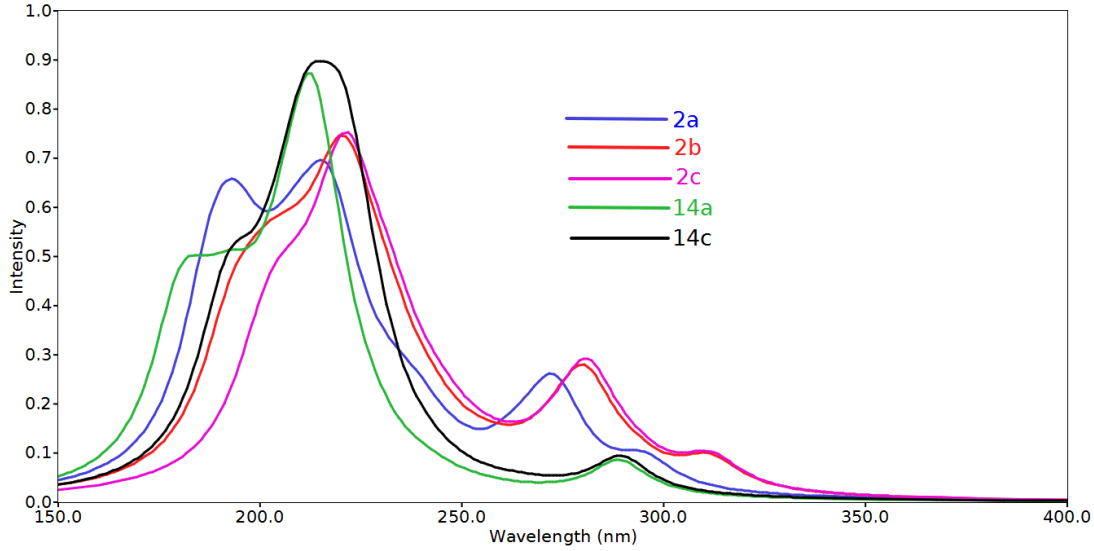

Fig. 3 The calculated electronic spectra of the studied compounds.

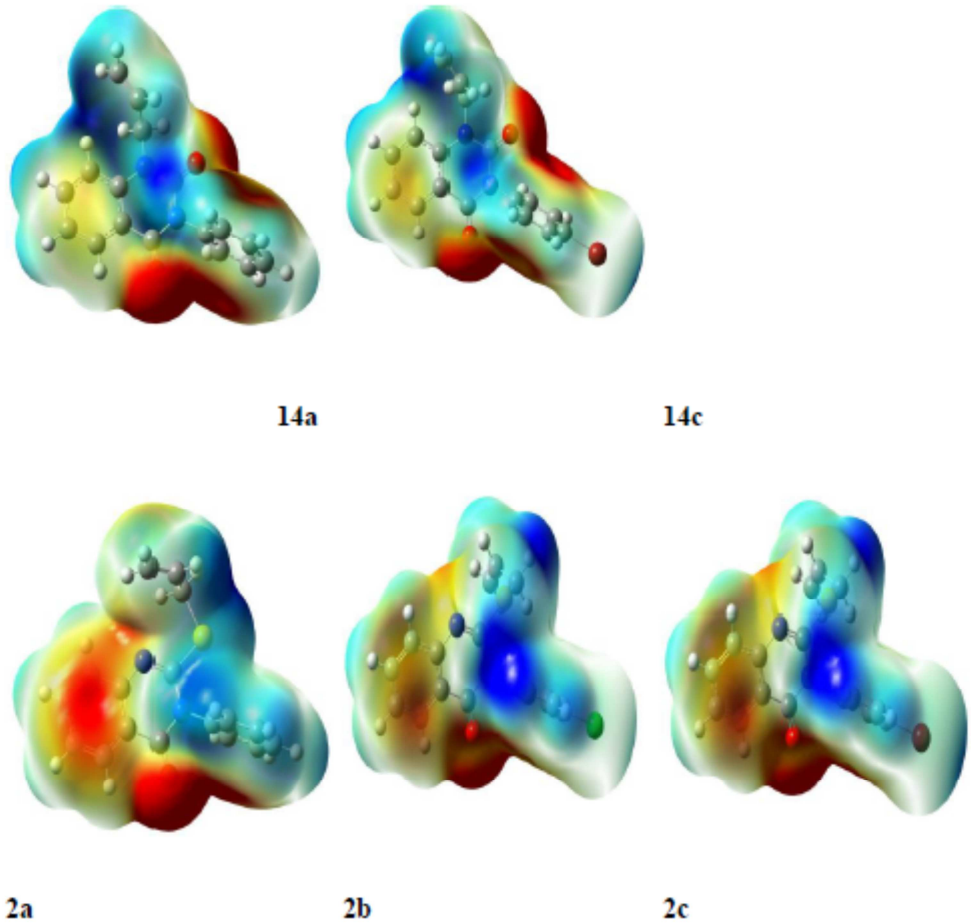

Fig. 4 Molecular Electrostatic potentials (MEP) mapped on the electron density surface calculated by the DFT/B3LYP method.

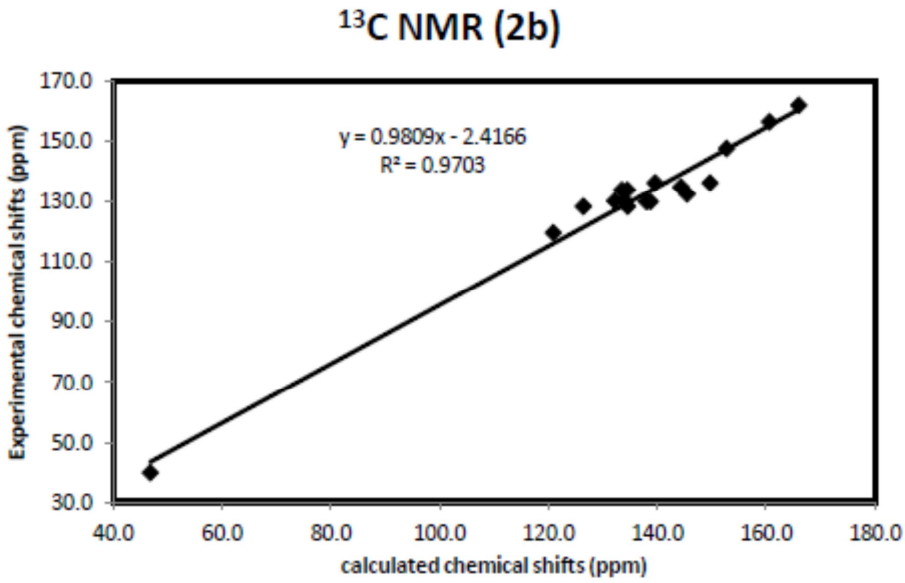

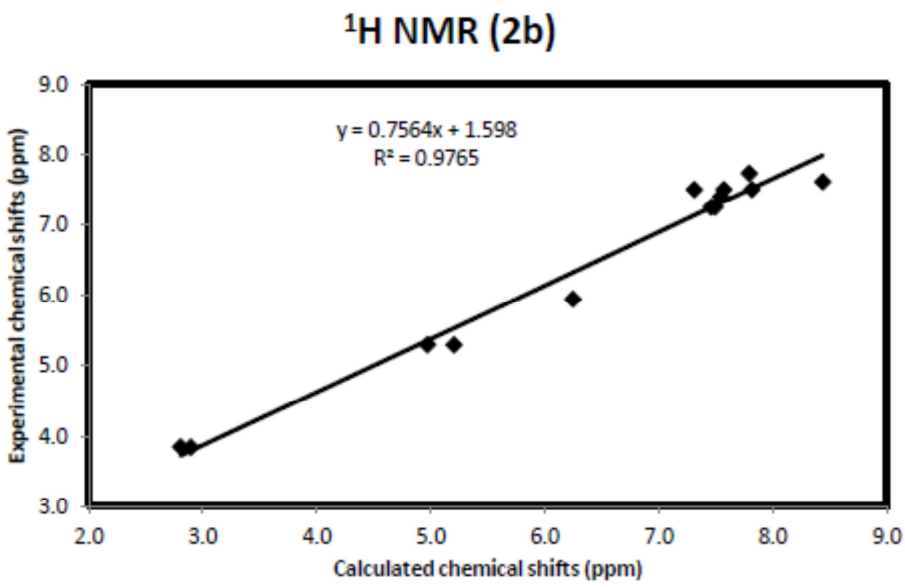

Fig. 5 Correlations between the experimental and calculated chemical shifts using the GIAO method for compound **2a**.

Highlights

- A new series of N- and S-alkylated quinazolines derivatives were synthesized.
- The 2-mercapto-3H-quinazolin-4-one, **1** goes via the S-alkylation.
- The quinazolin-2,4-dione, **12** favored the N-alkylation.
- Chemical reactivity and site selectivity of the reactants **1** and **12** were presented.
- The molecular structures, electronic and spectroscopic properties of the products were predicted.